Ignition Regime and Burn Dynamics of DT-Seeded D^{3}He Fuel for Fast Ignition Inertial Confinement Fusion

Y. Nakao, **K. Tsukida**, **K. Shinkoda**, **Y. Saito**

Department of Applied Quantum Physics and Nuclear Engineering, Kyushu University, 744 Motooka, Fukuoka 819-0395, Japan
e-mail contact of main author: nakao@nucl.kyushu-u.ac.jp

T. Johzaki, **K. Mima**

Institute of Laser Engineering, 2-6 Yamada-oka, Suita, Osaka University, Osaka 565-0871, Japan

Abstract. The feasibility of burning D^{3}He fuel in the fast-ignition inertial confinement fusion scheme is examined by paying special attention to the plasma heating processes by fusion-produced fast particles. Simulations have been made for a DT/D^{3}He pellet compressed to 2000 ~ 4000 times the liquid density. Newly included in the calculations is the transport of recoil ions generated by knock-on collisions of D-T neutrons and D-^{3}He protons. Although the ignition condition and burn properties are degraded by the inclusion of recoil-ion transport, it is still possible to obtain sufficient pellet gains (> 60) with realistic driver energy below 10MJ.

1. Introduction

Although D-^{3}He fusion is characterized by its requirement of increased confinement, higher operating temperature and yielding a lower power density compared with D-T fusion, it is considered to be of long range interest for its potential advantages of (a) low neutron generation and (b) efficient conversion of output fusion energy. In inertial confinement fusion (ICF), the use of pure D^{3}He fuel is impractical because of the excessive requirement on driver energy. A small amount of DT fuel as "igniter" is hence indispensable. As far as the central hot-spark ignition scheme is adopted, the driver energy still remains to be of excessive [1-4].

To reduce further the requirement on driver energy for D-^{3}He fusion, in previous papers [5] we proposed to adopt the fast ignition scheme [6]. The works showed that it may be possible to obtain sufficient gains (~100) with realistic driver energy below 10MJ. A crucial role of D-T neutrons in heating up the D^{3}He fuel was clarified. The importance of nuclear elastic scattering (NES) of D-^{3}He protons as a self-heating mechanism in D^{3}He plasma was also demonstrated.

In the above calculations, the energy depositions from neutron collisions and NES of energetic protons were treated as "local/instantaneous" processes, occurring at the same point and time at which the collisions take place; the transport (*i.e.,* slowing-down and diffusion) of recoil ions generated by these collisions was not solved there. Such a treatment may overestimate in some cases the plasma heating by fusion-produced particles. For accurate evaluation of the ignition and temporal evolution of thermonuclear burning, it would be important to consider the recoil-ion transport.

In this paper, we examine the ignition and burn properties of compressed DT/D^{3}He fuel targets by paying some special attention to the energy deposition process of fusion-produced fast particles. To grasp the ignition regime, first we show the contour map of the pellet gains and the output neutron energy fractions on the $\rho R_{Total} - \rho R_{DT}$ plane derived from the calculations neglecting the recoil-ion transport. Then, for a representative operating point in the $\rho R_{Total} - \rho R_{DT}$ plane, we show how the gain is degraded by inclusion of the recoil-ion transport.

2. Model Description

2.1. Collision processes and simulation code

The thermonuclear reactions occurring in DT/ D^3He plasmas are T $(d, n)^4$He, D (d, p)T, D (d, n) ^{3}He, and ^{3}He $(d, p)^4$He. The particles emitted from these reactions collide with the plasma species, depositing their energy. For charged particles, the dominant process is, of course, Coulomb scattering. However, in collisions of highly energetic particles (*e.g.*, 14.7-MeV protons), the contribution from nuclear elastic scattering (NES) becomes significant [7]; the stopping range of 14.7-MeV protons in D^3He plasmas is considerably shortened by NES. For ^{3}He or alpha particles, the NES effect is negligible. The transport of energetic protons was treated by the proton diffusion routine including NES. The neutron heating is also essential in the DT / D^3He fuel burning, and then we incorporated the updated multi-group neutron diffusion code into the FIBMET, a 2D fusion ignition and burning code [8].

The radiation transport is treated by a multi-group diffusion model. The processes considered here are bremsstrahlung, inverse-bremsstrahlung and Thomson scattering. The inverse-Compton scattering is not included.

2.2. Initial pellet condition and assumptions

Figure 1 illustrates the "initial" state of fuel in a DT/ D^3He pellet configuration. The pellet with a temperature of $T_i = T_e = 0.2$ keV was assumed to have been compressed to $\rho = 2000 \sim 4000 \, \rho_{Liquid}$ (*i.e.*, $320 \sim 640 \, g/cm^3$). Such a compression is, of course, not an easy task, but it is indispensable in order to burn D^3He fuel with reasonable driver energy.

The radiation temperature at the start of the calculation was set to be the same as bulk electron temperature. The size of external heating region was assumed to have a 30 micron spot diameter and $1.0 \, g/cm^2$ depth. The heating pulse duration was taken as 30 ps. The coupling efficiency from the implosion laser to the target core plasma was assumed as 10% and that from the heating laser to the imploded core as 30%. The heating laser intensity was taken as 3.33×10^{20} W/cm^2. The heating laser energy transferred to the compressed core is thus estimated to be 70.4 kJ.
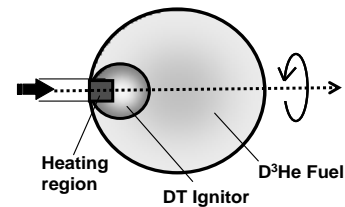

Fig.1. Initial fuel configuration

3. Result and Discussion

By incorporating the updated 2D diffusion codes for neutron and charged particles into FIBMET, we made burn calculations. The influence of energy deposition via recoil ions was also examined. The ignition condition was examined with a view to achieving pellet gains higher than 50 with a "moderate" total (*i.e.*, implosion plus heating) driver laser energy (< 10 MJ).

First we show the ignition regime derived from the calculations neglecting the recoil-ion transport. After that we examine how the inclusion of recoil–ion transport modifies the energy deposition profiles of fusion-produced fast particles and degrades the pellet gain of a representative operating point.

3.1. Ignition and burn properties—"local/instantaneous" deposition model

Figure 2 shows the pellet gains obtained for variously compressed fuel pellets ($\rho = 2000 \sim 4000\ \rho_{Liquid}$) as a function of the igniter mass M_{DT}. In this case, the total pellet mass M_{total} is fixed to 10 mg. It is seen that highly compressed pellet can save more fuel to obtain the same pellet gain compared to lowly compressed one.
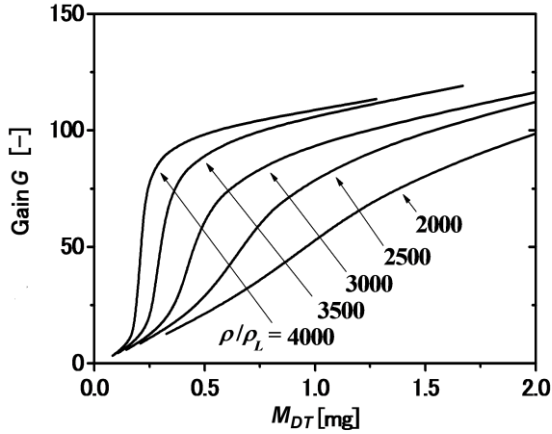
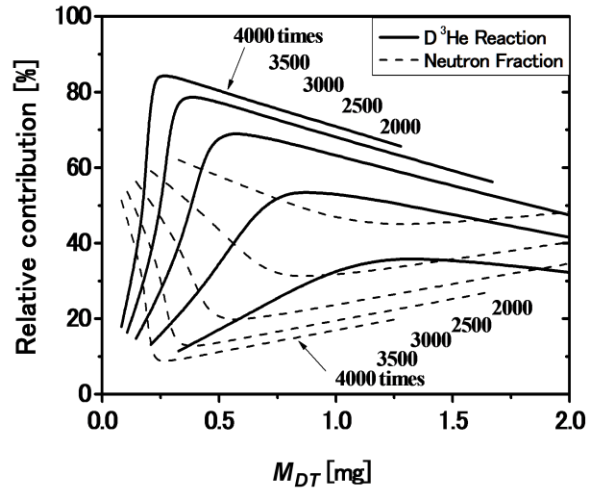Fig. 2. Pellet gains of variously compressed Pellets

Fig. 3. D-³He contribution to total fusion energy and neutron output fraction

Subsequently, we show the contribution of the D-^{3}He reaction to the total fusion output energy (full line) and the neutron output fraction F_N (broken line) in **Fig.3**. In the case that $\rho = 2000\ \rho_{Liquid}$, the D-^{3}He contribution remains at the 30% level, so the neutron output fraction is at least on the 40% level. In the case of $\rho = 4000\ \rho_{Liquid}$, we can make this fraction less than 10%.

Figure 4 illustrates the contour map of the pellet gain G as a function of the total mass M_{total} and the igniter mass M_{DT} for the case that $\rho = 4000\ \rho_{Liquid}$. There are also neutron output fraction curves in Fig. 4.
We can see that the pellet gain increases with increasing M_{DT}, so it can be said that at upper region of gain curves, the gain becomes larger.
Neutron output fractions become lower as they go inside of full lines, because a too little igniter cannot ignite the D^{3}He main fuel and a too large one increases the amount of D-T reactions.
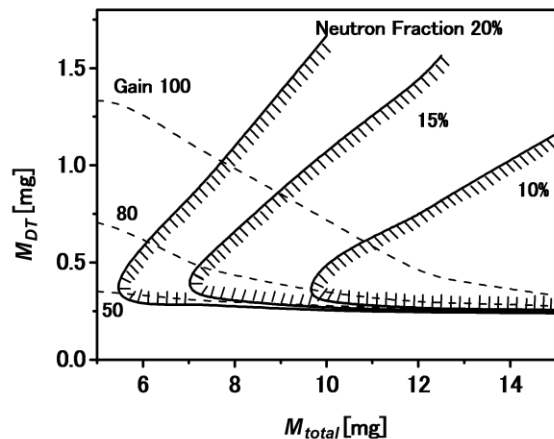
Fig.4. Contour map of pellet gains and neutron output fraction ($4000\ \rho_{Liquid}$).

Figure 5 reproduces the above pellet gain curves and a contour on which the fraction of neutron output energy $F_N = 10\%$ on the $\rho R_{Total} - \rho R_{DT}$ plane. At a representative point A ($\rho R_{Total} = 10.3 \text{g/cm}^2$, $\rho R_{DT} = 3.0 \text{g/cm}^2$ and $E_{driver} = 7.5 \text{ MJ}$), the pellet gain $G \geq 80$ and the neutron output fraction $F_N < 10\%$ are obtained. More than 80% of the fusion energy production is due to the D-^{3}He reaction.
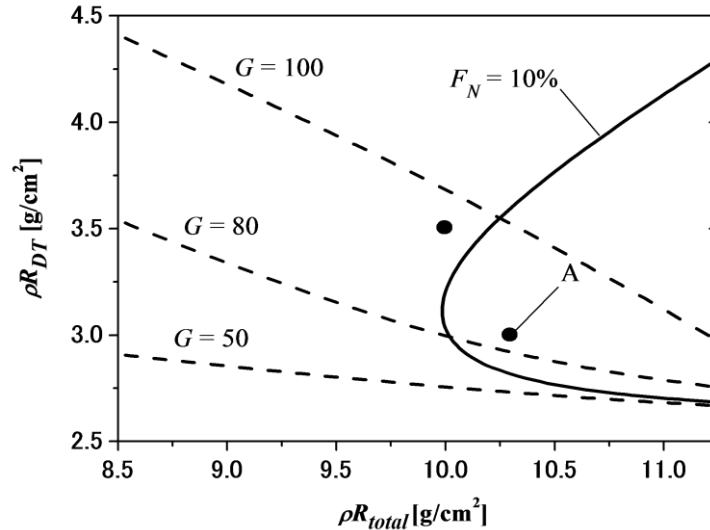

Fig. 5. Contour map of pellet gains and $F_N = 10\%$ (4000 ρ_{Liquid}).

3.2. Influence of recoil-ion transport

In the above calculations, the "local / instantaneous" model was used for the energy deposition from neutron collisions and NES; the recoil ion transport was not included. This energy deposition model overestimates the plasma heating by D-T neutrons and D^{3}He protons, by 10-20% depending on the plasma conditions. Inclusion of the slowing-down and diffusion of recoil ions should weaken the plasma heating because some of the recoiled ions would be lost from the plasma before slowing down.

We examine how the inclusion of recoil-ion transport influences the energy deposition profiles of 14.1-MeV neutrons and 14.7-MeV protons. To this end, we assumed a "stationary" plasma sphere homogeneously mixed with D (45%), ^{3}He (35%) and T (20%), and calculated the slowing-down and diffusion of these particles generating isotropically in the central region of the sphere. **Figure 6** shows the energy deposition profiles for 14.7-MeV protons. In this test calculation case, all the energies of source protons are deposited in the plasma sphere. When the "local / instantaneous" deposition model is used, the relative depositions to plasma ions and electrons are 23% and 77%, respectively. If we include the recoil-ion transport, these fractions change to be 10% and 90%.

In the case of 14.1-MeV neutrons, about 40% of the source neutron energies are lost out of the plasma sphere considered here. When the "local / instantaneous" deposition model is used, 62% of the source energies are deposited to the plasma ions. The rest (38%) is lost out of the sphere; deposition to the plasma electrons is 0%. In contrast, if we include the recoil-ion transport, the relative deposition to plasma ions decreases to 16%, while the deposition to plasma electrons becomes significant, 42%. The loss fraction also increases to be 42%.
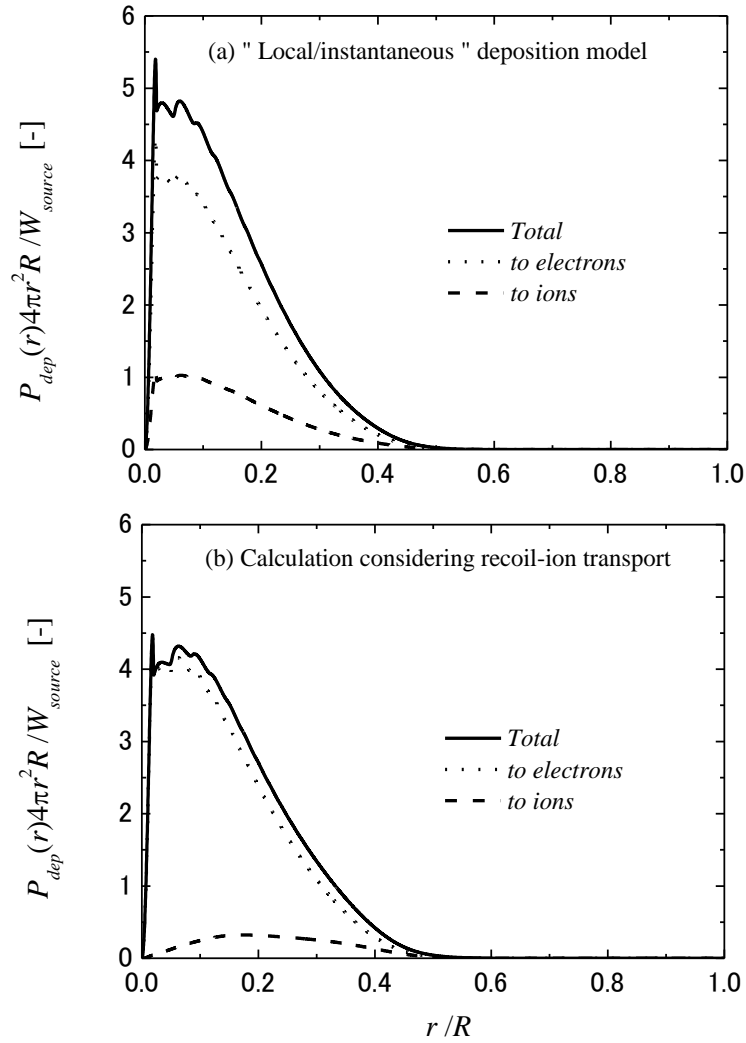
Fig. 6 Energy deposition profiles of 14.7-MeV protons ($\rho R = 10\,\mathrm{g/cm^2}$, $T = 20\,\mathrm{keV}$).

As is seen from the above calculations, if the energy depositions from neutron collisions and NES of protons are treated as "local / instantaneous" processes, the plasma heating (especially ion heating) by D-T neutrons and D-^{3}He protons in DT / D^{3}He system cannot be accurately treated. Burn simulations adopting this "local / instantaneous" heating model tend to overestimate the pellet gains.

The inclusion of recoil-ion transport weakens the plasma heating by fusion-produced energetic particles such as D-T neutrons and D-^{3}He protons. As a result, degraded pellet gains G would be obtained. The contour map of pellet gains and neutron output fractions shown in Fig. 5 hence should be modified. At present, however, we have no enough simulation results to accomplish this.

We made burn simulation including recoil-ion transport for one "initial" pellet condition same as that of point A in Fig. 5 ($\rho R_{Total} = 10.3\mathrm{g/cm^2}$, $\rho R_{DT} = 3.0\mathrm{g/cm^2}$, $\rho = 4000\,\rho_{Liquid}$; $E_{driver} = 7.5\mathrm{MJ}$). The pellet gain in this condition was estimated to be 65.

4. Concluding Remarks

We have discussed the ignition and burn characteristics of DT/D^3He pellet models in the fast–ignition ICF by assuming "initial" fuel state compressed to $2000 \sim 4000$ times the liquid density. Some special attention was paid to the energy deposition by fusion-produced fast particles. Although the ignition condition is degraded by inclusion of the recoil-ion slowing down and diffusions, the pellet gains still remains sufficient (> 60). To draw pellet gain curves and clear requirement on the driver energy, we need further simulations for various "initial" pellet conditions.

References

[1] G.H. Miley, in High Power Particle Beams (Proc. 6th Int. Conf., Kobe, 1986), Laser Soc. Jpn (1986) 309.
[2] T. Shiba *et al.*, Nucl. Fusion **28** (1988) 699.
[3] T. Honda *et al.*, Nucl. Fusion **31** (1991) 858; Y. Nakao *et al.*, Fusion Technol. **22** (1992) 66.
[4] M. Tabak, Nucl. Fusion **36** (1996) 147.
[5] T. Ohmura *et al.*, J. Phys.: Conf. Series **112** (2008) 022068; Y. Nakao *et al.*, Fusion Sci. Technol. **56** (2009) 414.
[6] M. Tabak *et al.*, Phys. Plasmas **1** (1994) 1626.
[7] Y. Nakao *et al.*, Nucl. Fusion **30** (1990) 143.
[8] T. Johzaki *et al.*, Proc. of 3rd Int. Conf. on Inertial Fusion Science and Applications (Monterey, 2003), edited by B.A. Hammel *et al.* (2004) 474.